AAEC/E 96

AAEC/E 96

AUSTRALIAN ATOMIC ENERGY COMMISSION

RESEARCH ESTABLISHMENT

LUCAS HEIGHTS

THE IRRADIATION BEHAVIOUR OF BERYLLIUM BASED DISPERSION FUELS – A PRELIMINARY IRRADIATION EXPERIMENT

by

G. L. HANNA

B. S. HICKMAN

R. J. HILDITCH

Issued Sydney, September 1962

UNCLASSIFIED

AUSTRALIAN ATOMIC ENERGY COMMISSION

RESEARCH ESTABLISHMENT

LUCAS HEIGHTS

THE IRRADIATION BEHAVIOUR OF BERYLLIUM BASED DISPERSION FUELS – A PRELIMINARY IRRADIATION EXPERIMENT

by

G. L. HANNA

B. S. HICKMAN

R. J. HILDITCH

ABSTRACT

The effects of fission fragment damage on vacuum hot pressed fuel specimens of (U Th) Be_{13} dispersed in a beryllium matrix were examined by irradiation in a predominantly thermal neutron flux. Damage equivalent to that caused by 4×10^{19} to 11×10^{19} fissions per cm^3 (depending on specimen composition) was achieved at temperatures between 435° and 530 °C.

All specimens increased in volume on irradiation. The increases ranged from 0.1 per cent. to 5 per cent., depending on the volume fraction of fuel phase and the number of fissions per cm^3. Some of the volume change – possibly up to 0.7 per cent. – was due to thermal effects alone.

Release of fission gases was as high as 2 per cent. in some cases and was generally higher than would be expected from recoil in specimens having no open porosity. The fractional release was greater in specimens which experienced a high volume increase.

Microstructures showed no significant change on irradiation. All specimens were slightly porous before irradiation and it is considered that the swelling of specimens was due to the growth of existing pores and that the release of fission gases was facilitated by an increase in open porosity.

CONTENTS

CONTENTS (continued)

1. INTRODUCTION

One of the fuel systems being examined for the Australian high–temperature–gas–cooled reactor is a dispersion of the beryllides of uranium and thorium in beryllium. The properties of such a fuel may alter during irradiation owing to the following phenomena:

(i) Accumulation of fission products.

(ii) Production of gases by the (n,2n) and (n,α) reactions in beryllium.

(iii) Lattice displacements caused by fission fragment and fast neutron bombardment.

The main advantage of a dispersion–type fuel is that provided the fuel particle size and volume fraction of fuel phase are chosen correctly (White et. al., 1957), fission fragment damage is concentrated in or near to the fuel particles and the matrix is left substantially free of damage by fission fragments.

For the initial experiments it was decided to study fission fragment damage by irradiating fuel dispersions in an essentially thermal flux, and fast neutron damage by irradiating beryllium in a fast neutron flux. Preliminary results from the beryllium metal irradiation programme reported by Hickman (1961) indicate that gas formation by the (n,2n) and (n,α) reactions may seriously affect the properties of beryllium after high doses and may be the main factor determining fuel element life while atomic displacements should be unimportant at irradiation temperatures above 100 °C. Combined fission fragment and fast neutron damage will be studied in the later stages of the programme by irradiating fuel specimens in a hollow fuel element position.

This report describes the first of the series of experiments designed to investigate fission–product damage. Specimens consisting of solid solution uranium – thorium beryllide particles dispersed in beryllium were irradiated in rig X–11 in a 4V position in HIFAR. The flux was predominantly thermal and damage due to the fast neutron reactions was virtually absent. Factors leading to the choice of the fuel specimens were discussed in detail by Hickman (1962).

Eight pairs of specimens were irradiated. Details are given in Table 1.

1.1 Scope of the Experiment

The variables chosen for the experiment were as follows:

(i) Composition:

The heavy metal : beryllium ratio ranged from 31 : 1000 to 31 : 4000 in four steps.

When the experiment commenced only preliminary surveys had been made of the fissile–fertile – moderator ratios likely to be suitable for an H.T.G.C. reactor. These surveys indicated that the uranium : thorium : beryllium ratio would probably be in the range 1 : 30 : 1000 to 1 : 30 : 4000.

To retain the advantages of a dispersion type fuel and to allow fabrication of the fuel by extrusion or rolling, the volume fraction of the dispersed phase should not exceed 0.25 – 0.30 which is equivalent to an atom ratio of 1 : 30 : 2000. However, as the specimens for this test were to be fabricated by vacuum hot–pressing, the composition range was extended down to an atom ratio of 1 : 30 : 1000 to cover the full range of interest.

(ii) Irradiation Temperature:

The experiment was designed to cover the temperature range 500 – 700 °C.

(iii) Burn–up:

Fission product damage equivalent to 100 per cent. burn–up* was planned for all specimens except two (numbered 29 and 30) which were to be taken to an equivalent burn–up of about 200 per cent. To achieve these equivalent burn–ups in a reasonable time the damage rate was accelerated by replacing some of the thorium by uranium. It was considered that this would not significantly affect the irradiation behaviour of the material.

* see note, top of page 2 .

*NOTE

Throughout this report the term "equivalent burn-up" will be used to relate the burn-up in the test specimens to that in the fuel mixtures of actual reactor systems. The term is defined by the expression:

$$\text{Equivalent burn-up, per cent.} = \frac{N_f \times 100}{N} ,$$

where N_f is the number of atoms fissioned in the test specimen and N is the number of U-235 atoms in a fuel mixture having the same heavy metal : beryllium ratio, but a uranium : thorium ratio of 1 : 30.

(iv) Fuel Particle Size:

The fuel particle size chosen for the majority of specimens was 100 – 150 microns which is the optimum size indicated by the theory developed by White, Baird, and Willis (1957). In two specimens (numbered 17 and 18) a particle size of about 10 microns was used to investigate the case where a substantial proportion of the matrix would be subjected to fission product damage.

2. EXPERIMENTAL PROCEDURES

2.1 Specimen Preparation

The materials used in the preparation of the test specimens were calcium-reduced uranium enriched to 93.4 v/o, calcium-reduced thorium powder, and Pechiney electrolytic beryllium powder. The major impurities in these materials are listed in Table 2.

Full details of specimen fabrication were reported by Hanna, Turner, and Smith (1961). To obtain the accelerated burn-up three batches of solid solution beryllides were prepared and referred to as compositions A, B, and C. They had the following uranium to thorium atom ratios:

Composition A 12 U : 19 Th

Composition B 14 U : 17 Th

Composition C 24 U : 7 Th

These solid solutions were prepared by reacting the constituent metal powders at 1550 °C under pressure of 1 t.s.i. in a graphite die. The product was a dense compact which was crushed and screened to give particles of the required size.

The dispersion specimens were fabricated individually by vacuum hot-pressing mixtures of the appropriate beryllide powder and beryllium metal powder. Densities close to theoretical were achieved at 800 °C and 15 t.s.i. by a double compaction process in which the compact was inverted in the die between the first and second pressings. Specimens were brought to the final dimensions of 0.9 cm diameter by 1.8 cm long by machining to a tolerance of 0.0025 cm.

Optical measurements of the beryllide particles are given in Table 3. Particle shape differed markedly from the ideal spherical or equiaxed shape as the longest dimensions were sometimes 3 or 4 times the diameter of the ideal 100 micron sphere.

Chemical analysis of the batches of beryllide (Table 4) showed that none were exactly stoichiometric; batches of compositions A and C were deficient in beryllium (corresponding to $MBe_{12.8}$ and $MBe_{12.45}$ respectively) whereas the batch of composition B was beryllium rich (corresponding to $MBe_{13.45}$). The uranium to thorium ratios in each batch also departed from the specified figures and this suggests that there was some heterogeneity within the materials.

2.2 Pre-Irradiation Measurements

Prior to irradiation, the dimensions of all specimens were measured to an accuracy of ±0.00025 cm Volumes and densities were determined by displacement in n-octyl alcohol both before and after vacuum impregnation; however no significant differences were observed.

Although all specimens were fabricated individually, it was not possible to examine each one metallographically before irradiation or heat treatment. However one spare specimen in each group was available and provided examples of the as-fabricated microstructures. Photomicrographs of these are shown in Figures 6 to 11. The examination showed that some fuel particles cracked during hot-pressing, and that poor wetting resulted if there was a cluster of fuel particles. No gross segregation of fuel particles was observed but groups of 2 to 5 were often found in which particles were very close and sometimes in contact. There was some porosity in the microstructures, particularly at clusters of particles.

All specimens were photographed before insertion in the irradiation rig. One specimen of each heavy metal : beryllium ratio is shown in Figure 4.

2.3 Rig Design and Assembly

The specimens were irradiated in a standard A.A.E.C. 4V fuel rig in a four inch vertical hole (the 4V-1) hole). Nuclear heating provided the designed specimen temperature and the rig was cooled by the reactor heavy water.

A general arrangement of the rig is shown in Figure 1. It consisted of two side-by-side aluminium tubes which dipped into the reactor heavy water and were protected by a perforated outer aluminium tube. Eight test specimens, double canned in stainless steel, were loaded into each of these tubes so that duplicate specimens occupied the same positions in each stringer. A schematic cross section of part of one of these stringers, showing the arrangement of the inner and outer specimen cans and the aluminium former into which the latter fitted, is shown in Figure 2. The outer stainless steel can was a push fit in the aluminium former which in turn was a push fit in the outer aluminium containing tube.

The width of the helium-filled gas gap between the two cans was chosen so that nuclear heating would raise the temperature of the inner can to the desired value during operation. The heat outputs of each specimen were calculated using flux data for a simulated 4V rig obtained during low power operation of HIFAR, Connolly and McKenzie (1960); flux depression in the specimens was calculated by the empirical method due to Lewis (1954). Individual heat transfer calculations to arrive at the gas gap dimensions were made for each can assuming that transfer occurred only by conduction and radiation and using temperature distribution data obtained in tests on a prototype out-of-pile rig. Mineral-insulated stainless-steel-sheathed thermocouples were fitted into thermocouple pockets in each end of the specimen cans. The thermocouple pockets also served to position the inner can.

Each fuel specimen sat loosely in a stainless steel cup which was sufficiently large to permit a considerable amount of swelling of the specimen. Thermal-flux monitors in the form of 5 mg of cobalt wire cemented to an alumina tube were sealed in the space between the two stainless steel cans. The inner cans were filled with high-purity double-distilled sodium in a pure helium atmosphere in a dry box; the sodium level was carefully adjusted until level with the top of the specimen and the end cap was welded in position under a helium pressure of one atmosphere without removing the cans from the dry box. After leak testing, which involved heating to 500 °C for 48 hours, the cans were radiographed to check the sodium level. The inner cans were then loaded into the outer cans, and welding was carried out in the dry box under one atmosphere of helium. Finally the cans were fitted with thermocouples, assembled into stringers, and loaded into the rig. All thermocouples were checked against a standard at 500 °C before use and shown to be within ± 2 °C of the correct value.

Finally, the whole assembly was attached to a shield plug (Figure 1) provided with service tubes and purge lines (to purge the space between the outer can and the aluminium containing tube). Thermocouples were connected to compensating leads at the top of the plug and the temperatures of all specimens were recorded on multi-point potentiometric instruments.

Although two thermocouples were provided for each specimen, the top one was intended solely as a safeguard against failure of the lower couple. It was not expected to give a reliable measurement of the specimen temperature as it only just broke the surface of the molten sodium.

2.4 Rig Operation

2.4.1 First approach to power

After loading the rig into the reactor, the space between the outer stainless steel can and the aluminium containing tube was purged with helium to a pressure of 1 p.s.i. above atmospheric. When

the reactor reached a steady power of 10.2 MW it was found that most of the specimen temperatures were lower than the designed irradiation temperatures by 100 to 200 °C. The rig was immediately purged with carbon dioxide and temperatures rose by 30 to 50 °C. Although the specimen temperatures were still low (by 70 to 160 °C) after the carbon dioxide purge, the experiment was continued.

2.4.2 Steady state operation

The temperature histories of the specimens, as indicated by the lower thermocouples, are shown in Figures 3a and 3b. In general, temperatures fell slowly under steady state reactor operation but four specimens (numbered 1, 2, 17, and 18) showed a fairly persistent temperature rise. The progressive fall in temperature is believed to be due to depletion of U–235 but the reason for the temperature rises in the four specimens mentioned is not known.

After irradiation had been in progress for 2100 hours, carbon dioxide was detected in the helium blanket of the reactor core. As it was thought that this may have been due to a leak in the rig, the purge gas was replaced by helium. The subsequent rates of fall of specimen temperatures were greater than before but on re–purging with carbon dioxide at 2450 hours (total in–pile time), the temperatures increased by 10 to 25 °C and remained steady until the rig was withdrawn from the reactor.

The rig was in the pile for a total of 2600 hours during which time twelve shut–downs occurred.

The specimen temperatures as recorded by the lower thermocouples are summarised in Table 1. The table gives the designed irradiation temperatures, the extremes of temperature actually experienced during irradiation, and the estimated mean temperature during irradiation.

2.4.3 Relationship between indicated and actual temperatures

It must be emphasised that the temperatures recorded by the lower thermocouples were lower than the true specimen temperatures.

Although sodium film–boiling is unlikely to occur adjacent to specimens having the heat ratings found in this experiment, surface effects may have been operative which would give rise to specimen temperatures greater than those indicated by the thermocouples. A recent evaluation (Hickman et al. 1961) indicated that longitudinal temperature gradients of 5 – 10 °C/cm existed along the surface of specimens during irradiation (specimens hotter at the top) and that the surface temperatures at the bottom may have been 10 to 15 °C higher than the thermocouple temperature.

Radial temperature gradients will also have been set up during irradiation and these will have been between 6½ °C for the lowest rated specimens and 21 °C for the most highly rated specimens, (assuming the unirradiated value for the thermal conductivity).

It appears therefore, that during steady state operation, the temperature differences between the thermocouple and specimen surface at its half height (taking a mean figure of 20 °C) and between the specimen surface and centre resulted in a total difference of 26 to 40 °C between the temperatures at the specimen centre and the lower thermocouple. Furthermore, Hickman et al. (1961) suggested that for a short period during reactor start–up (less than one minute), specimen temperatures may have been a further 30 – 40 °C above this estimated maximum.

2.5 Post–Irradiation Examination

At the end of the irradiation period, the rig was unloaded and stored for several weeks in a HIFAR storage block. It was dismantled in the high–activity handling cells by cutting open the outer aluminium tube and withdrawing the specimen cans from the formers. The outer specimen cans were removed by milling and the cobalt monitors extracted. Visual examination of the inner cans through the cell windows revealed no evidence of distortion or sodium leakage.

The amounts of fission gases released during irradiation were measured by piercing the inner cans in an evacuated system of known volume and measuring the pressure rise. Gas composition was determined by mass spectrometry. The can was raised to 150 °C during piercing, to melt the sodium and release any entrapped gas. Only nine of the sixteen cans were successfully sampled.

After removing the specimens from the inner cans sodium adhering to the specimen surfaces was removed by washing in ethyl alcohol and then water, but where this did not give satisfactory cleaning, specimens were scrubbed with a soft wire brush.

Specimens were examined and photographed at a magnification of 2 to 15 times using a stereo-periscope. Dimensions were measured using a dial gauge in conjunction with slip gauges, and volumes were determined by displacement in n-octyl alcohol, both without and with a preliminary impregnation under vacuum. Specimens selected on the basis of volume change during irradiation (numbered 2, 6, 17, 21, 22, 25, 29, and 30, see Table 7) were slit into transverse and longitudinal sections and examined by microscopy. Photomicrographs of the specimens are presented in Figures 12 - 19.

The procedure for metallographic preparation comprised the following steps:

(i) Grinding on 120, 220, 320, 400, and 600 grade silicon carbide papers on a Buehler automet machine.

(ii) Polishing on a Syntron vibratory polishing machine for about 15 hours using nylon cloth and a medium grade alumina polishing compound.

(iii) Etching for 20 seconds in a solution of 2½ per cent. hydrofluoric acid, 5 per cent. nitric acid, in absolute alcohol.

Some difficulty was experienced in etching the irradiated specimens and some of the photo-micrographs show stains on the fuel particles. It is thought that this difficulty arose from the volatility of the etchant (and therefore rapid changes in composition in the heavily ventilated cell), and the solu-bility of the mounting plastic in the etchant, with consequent smearing of the plastic over the specimen surface.

The burn-up in each specimen was calculated from HIFAR flux data (obtained from measure-ments made during low power operation) and from flux data calculated from gamma spectrometry on the cobalt monitors. In each case, flux depressions in the samples were estimated by the empirical method developed by Lewis (1954).

A more direct determination of the burn-up in specimens 7 and 30 was made by radiochemical determination of the fission yield of Cs-137 and mass spectrometric determination of uranium isotope dilution (ratio of U-235 to U-238).

2.6 Out-of-Pile Control Specimens

One specimen of each composition defined in Table 1 was sealed with sodium into a stainless steel can in the same way as the irradiated specimens. They were subjected to a heat treatment which followed all but the minor variations (less than 20 °C) in the thermal history of selected specimens in the irradiation rig (Specimens 1, 5, 7, 9, 17, 21, 25, and 29). At the completion of the heat treatment all specimens were examined for dimension and density changes and then prepared for metallographic examination in the same way as the irradiated specimens.

3. RESULTS

3.1 Burn-up Determination

Equivalent burn-ups calculated from flux data obtained at low power operation of HIFAR were supported with fair consistency by the gamma spectrometry of the cobalt monitors. However, the results of the chemical determinations (Cs-137 content and uranium isotope dilution analysis) on the irradiated specimens 7 and 30, were very high and must be considered suspect.

The results of the various determinations are listed in Table 5. As was intended, specimens 1 to 26 all underwent an equivalent burn-up of about 100 per cent. and specimens 29 and 30 experienced an equivalent burn-up of about 200 per cent.

3.2 Fission Gas Release

The quantities of gaseous fission products released from the specimens are shown in Table 6. These are quoted as actual quantities of each isotope found in each can and as percentages of the total amount of each isotope produced by fission in the specimen and released into the cans. The latter figures were calculated using the burn-up values determined from γ spectrometry of the cobalt monitors.

The amounts of gases released – both actual and percentage – tended to increase with the uranium content of the specimen and with the burn-up. The highest release was observed in the most concentrated dispersions (31 : 1000 heavy metal : Be ratio) taken to an equivalent burn-up of 100 per cent; in this case the release of the several isotopes varied from 1.5 to 2.5 per cent. In specimens taken to an equivalent burn-up of 200 per cent. (specimens 29 and 30) the release varied from 0.85 to 1.6 per cent.

The lowest release was observed in specimen 6 (31 : 3000 heavy metal : beryllium ratio) and not in specimen 1 which was the most dilute of the specimens successfully sampled.

3.3 Macro-examination

Macro-examination at magnifications of 2 – 15 times revealed little distortion in any specimens. The original geometric shape was well preserved, except for slight rounding of the edges, and no cracks were visible. The original machining marks could be seen on the surface of most specimens.

There appeared to have been some reaction between the specimen material and the liquid sodium used as the heat transfer medium. The reaction products appeared as a black scale adhering to the surface after washing in alcohol and water. The specimens had a slightly pitted surface apparently resulting from the surface reaction. The lower end of the specimens appeared to be the more affected.

Some specimens appeared to be impregnated with sodium. Examination of specimen 26 some weeks after the initial examination indicated that further deterioration of the metal surface had occurred as a result of continued reaction with residual sodium. This had led to increased pitting of the specimen surface and ejection of material from the matrix.

The surface defects produced by the attack varied from specimen to specimen. In some cases the roughening was uniform over the whole specimen but in others was more isolated and gave the impression of deeper pitting. A photograph of one of the worst affected specimens (number 25) which showed uniform attack, is shown in Figure 5b.

3.4 Dimension and Density Changes

The dimensions and densities of the specimens before and after irradiation are shown in Table 7. Density changes calculated from the dimension changes and those obtained by the displacement method after impregnation are both shown. Densities measured before impregnation did not differ significantly from the values after impregnation.

The changes in both dimensions and density increased with increase in the volume fraction of the dispersed phase (and therefore with increase in the number of fissions per unit volume of specimen), and with equivalent burn-up at constant composition. Volume changes were the result of a general swelling, as the specimen diameters and heights increased to similar extents.

Density decreases were between 0.1 and 1.2 per cent. in the more dilute specimens (31 : 4000 and 31 : 3000 heavy metal : beryllium ratios) and increased to about 5 per cent. in the most concentrated specimens (31 : 1000 heavy metal : beryllium ratio). Specimens 29 and 30 (31 : 3000 heavy metal : beryllium ratio) which were taken to an equivalent burn-up of 200 per cent. suffered density changes of 4.7 and 1.2 per cent. respectively and there is some suggestion that swelling in specimens 5 to 10, all having the same heavy metal : beryllium ratio as specimens 29 and 30. increased with burn-up.

Specimens 17 and 18, which had a heavy metal : beryllium ratio of 31 : 3000 but contained fine intermetallic particles (nominally 10 micron diameter), suffered density decreases of 3.1 and 2.5 per cent. respectively. These were considerably higher than in specimens of the same heavy metal : beryllium ratio which contained coarse intermetallic particles (nominally 100 to 150 microns diameter).

3.5 Metallographic Examination

Metallographic examination revealed no significant changes in the microstructure of any of the specimens examined. There was some evidence of porosity and cracking in the fuel particles but not to any significantly greater extent than that present in as-pressed, unirradiated specimens. Examination of the beryllium matrix under polarised light revealed no change in the grain structure and no evidence of damaged zones around the fuel particles.

Particular attention was given to the amount of porosity in the microstructures. Specimens 2 and 6 (Figures 12 and 13), which suffered only slight volume increases, showed little porosity compared with the other specimens which suffered larger volume increases. However, the location of the pores was very similar in all specimens.

Porosity could be divided into four types on the basis of location, as follows:

Type 1 Small, roughly spherical, pores within some fuel particles.

Type 11 Occasional pores at the boundaries of fuel particles which were well separated from other particles (Figure 16a).

Type 111 Severe porosity between fuel particles in close proximity to one another (Figures 17a and 17b).

Type IV Porosity within the beryllium matrix (Figures 13a and 13b).

Porosity of all four types was found in all specimens but that within the beryllium matrix was most prevalent in concentrated dispersions, and appeared to be the result of poor compaction during specimen preparation. No quantitative metallography was done to determine the amount of porosity, but there was an obvious correlation between the amount of porosity and the volume increase during irradiation.

Several of the specimens showed variations in the microstructure of the fuel particles. Some particles contained a large number of oxide inclusions (Figures 12 and 13) and some a number of pores (Figure 19) but others were quite free of any inclusions or porosity (Figure 16). However, no differences in behaviour of these various types of particles were observed nor was there any difference in the porosity distribution around them.

3.6 Out–of–Pile Control Specimens

Dimension and density changes which occurred on heat treatment of the control specimens are listed in Table 8. Dimension increases varied from 0.02 to 0.44 per cent. and density decreases from nil to 0.7 per cent. The observed changes were quite random and showed no apparent correlation with heat treatment temperature, volume fraction of dispersed phase, or composition of the intermetallic compound.

Microstructures of the control specimens were similar in all respects to those of the irradiated specimens (see Section 3.5). Hence no photomicrographs are included.

Attack by sodium on the specimens was very slight and amounted only to a discoloration of the surface and occasional slight pitting. A typical surface (specimen 27) is shown in Figure 5 where it is compared with that of an irradiated specimen of the same composition and thermal history.

4. DISCUSSION OF RESULTS

4.1 Relationship Between Actual and Indicated Temperatures

As indicated in Section 2.4.3, it was estimated that specimen centre temperatures were 26 to 40 °C higher than the thermocouple temperatures. Examination of the temperature recorder charts also showed that transient temperature peaking occurred as the reactor reached full power on start–up. However, the frequency at which the individual thermocouples were monitored was too low to permit estimation of the true peak temperatures.

It is doubtful whether the transient peaks and the estimated temperature errors have a great bearing on the interpretation of the results of the experiment. Neither the matrix nor the beryllide compounds undergo phase transformations below 1200 °C and the homogeneity limits of the beryllides are not known to change with temperature. One possible effect is an enhancement of diffusion rates which could lead to reaction of free uranium (or thorium) with the beryllium matrix, and the release of fission product gases at rates slightly greater than expected at the indicated temperatures. A second possible effect is a more rapid rate of swelling owing to a decrease in the mechanical strength of the matrix at the higher temperature.

It is considered that the estimated errors are too small to have any obvious effect on the diffusion controlled processes but the mechanical properties of the beryllium may be significantly different at the actual specimen temperature and may result in higher swellings than would be encountered at the indicated temperatures.

4.2 Burn–up Determination

With only two exceptions (specimen pairs 7–8 and 17–18), close agreement was found between the burn–up in duplicate specimens as calculated from the cobalt monitor activities. This suggests that these results are, in general, reliable but the disagreement between the pairs referred to above remains unexplained.

The very high values obtained from the Cs–137 analysis are also without explanation. An accuracy of only 90 per cent. is claimed for these values but even this cannot account for the discrepancy with the other methods.

The results of the isotope dilution analysis are being checked by repeat analyses but results are not yet available. Whittem (1961) showed that very slight contamination of the analysis sample with natural uranium can lead to surprisingly high results (e.g. 100 p.p.m. added to uranium of 93 V enrichment gives a 2 per cent. error in the burn–up expressed in atomic per cent.). It has been established by analysis of an unirradiated specimen that no contamination occurred before irradiation. However the possibility that it occurred during remote handling after irradiation cannot be ruled out. It is, perhaps, significant that specimen 7, the first to be sampled and therefore the one more prone to contamination, gave the higher result.

4.3 Dimension Changes

Metallographic examination established that the swelling of specimens could only have been due to increases in porosity. However, because of the variable distribution of porosity within individual specimens it was not possible to establish, in any quantitative way, which regions of the compacts yielded the extra porosity. The amounts of porosity within the fuel particles and the beryllium matrix were not obviously changed by irradiation. The number of pores at the boundaries of well separated particles may have increased slightly on irradiation but it was not possible to detect any change in the number or volume of pores between particles in close proximity. However, changes of five per cent. and less are difficult to detect metallographically where porosity distribution is non–uniform; many areas must be examined if an accurate result is to be obtained.

The fact that the unirradiated control specimens swelled during heat treatment demonstrated that some of the swelling in irradiated specimens was due to temperature effects alone. The random variation in swelling of control specimens indicates that temperature induced density changes of at least 0.7 per cent. should be allowed for in all irradiated specimens which swelled by more than this amount.

Swelling owing to temperature effects may be due to three factors:

(i) Nucleation of gases dissolved in the specimen and the subsequent growth of pores.

(ii) Reaction of free uranium or thorium with beryllium from the matrix.

(iii) Reaction of the specimen with the sodium heat transfer medium.

Although gas analyses were not done on either the beryllium or beryllide compounds used in these specimens, W.J.Stuart (private communication) found that beryllium powder from the same source does contain up to 0.8 $cm^3\ g^{-1}$ of hydrogen and smaller amounts of other gases. It has been observed that most of these gases are removed during vacuum hot pressing at 700 °C and the same will hold true for the compaction conditions used in the preparation of specimens for this experiment. It is possible however, that residual small amounts of gas trapped at fuel particle boundaries exerted sufficient pressure to make the specimens swell.

Severe swelling occurs when uranium and thorium beryllides are prepared from their constituent metal powders (Williams and Jones 1956). It is possible, therefore, that free uranium or thorium in dispersion specimens may result in swelling when it reacts with the free beryllium. This phenomenon may

partially account for the temperature induced swelling of all specimens except 17, 18, and 19, since these all contained beryllide deficient in beryllium. However, in specimens 17, 18, and 19 the beryllide contained an excess of beryllium, and swelling from this source would not be likely; nevertheless the unirradiated sample (No. 19) expanded by 0.4 per cent. It should be noted that although chemical analysis showed the beryllides to be of non-stoichiometric composition, metallographic examination of as-fabricated specimens did not reveal any free uranium, thorium, or beryllium within the fuel particles.

The apparent reaction of the irradiated specimens with sodium is not understood, but the good condition of the unirradiated control specimens indicates that either the reaction was accelerated by irradiation or that higher purity sodium was used for the control specimens (the cans were filled on different days). The specimens were not sufficiently porous for deep penetration of the sodium to have occurred but the microstructure of regions at and immediately below the surface was no different to that of the centre regions. It is considered that the surface attack made very little contribution to the dimensional changes of the irradiated specimens but, as discussed below in Section 4.4, it could have brought about an increase in the release of fission products owing to the ejection of fuel particles from the specimen surfaces.

To summarise, it is doubtful whether sodium or free uranium or thorium was responsible for the temperature induced swelling; the most likely cause appears to be gases which were dissolved or entrapped in the specimens prior to, or during, fabrication. It appears however that irradiated specimens of heavy metal : beryllium ratios of 31 : 2000 and 31 : 1000 swelled more than can be accounted for by heat treatment effects. This extra swelling may have been due to the expansion of existing pores by pressure exerted by fission gases which had diffused into them.

4.4 Fission Gas Release

Fission gas release showed an expected increase with the fission concentration within the specimen. This is most conveniently demonstrated in Table 9 which lists the total volume of gas released into the specimen can and the number of fissions per unit volume of specimen. The table also demonstrates that, in specimens of the same composition and fission concentration, the amount of released gas increased with increase in the change of density – that is, with increase of porosity. This supports the view that porosity increases were brought about by the build-up of pressure of gases within the pores; consequent swelling of the pores seems to have led to interconnection of some of the pores and enabled diffusion of gas to the specimen surface.

It is most probable that the unexpectedly high fission gas release was due in part to the surface degradation brought about by sodium attack; particles ejected from the surface by the reaction would subsequently release fission products into the cans. However, with the largest group of specimens of the same composition (numbered 5 to 10), it was difficult to assess truly the relative extent of surface attack and hence the importance of this factor in the release of fission gases.

5. CONCLUSIONS

If the envisaged operating temperature of the H.T.G.C. reactor is in the range of 600 to 700 °C, the usefulness of this first irradiation test of the $(U,Th)Be_{13}$ – beryllium fuel system is limited by the failure to achieve irradiation temperatures greater than 530 °C. However the results are helpful in providing a basis for speculation on the behaviour of such fuels at the likely operating temperature.

The swelling of specimens and release of gaseous fission products were generally greater than would be expected from a dispersion type fuel. It would be expected that the behaviour of similarly prepared specimens at higher temperatures would be even less favourable.

The swelling was due in part to heat treatment effects; and in dispersions of low concentration, could have been due entirely to thermal effects. Thermally induced swelling is thought to be due to faults of specimen preparation – for example, to entrapped or dissolved gases or non-stoichiometric beryllides – and stricter control of composition and fabrication techniques would probably improve dimensional stability.

The fission gas retention of hot pressed specimens was not good but the results indicate a correlation between gas release and the swelling of the specimen. Improved gas retention would be expected if the swelling could be reduced by removing the causes of thermally induced swelling. Canning of the fuel would, of course, reduce the release of fission gases but it is doubtful whether a can would significantly reduce swelling.

6. ACKNOWLEDGMENTS

Grateful acknowledgment is made to the following for assistance with the experiment: Mechanical and Electrical Design Group for the rig design; Reactor Operations Section for operation of HIFAR and logging of specimen temperatures; members of the Irradiation Group for rig assembly and post–irradiation examination; Analytical Chemistry Section for chemical analyses, and the Physical Metallurgy Group for preparing photomicrographs of unirradiated specimens.

7. REFERENCES

Connolly, J.W., and McKenzie, C.D., (1960). – AAEC/TM64.

Hanna, G.L., Turner, D.N., and Smith, P.D., AAEC/TM113.

Hickman, B.S., (1962). – AAEC/TM139.

Hickman, B.S., Smith, R., Hilditch, R.J., and Mercer, W.L., (1961). – AAEC/E 79.

Hickman, B.S., (1961). – "The Effects of Neutron Irradiation on Beryllium Metal". Conference on the Metallurgy of Beryllium, Inst. of Metals, London, 1961.

Lewis, W.B., (1954). – Nucleonics 12 (10), 31.

Williams, J., and Jones, J.W.S., (1956). – AERE M/R 1974.

White, O.W., Baird, A.P., and Willis, A.H., (1957). – KAPL 1909.

Whittem, R.N., (1961). – Internal A.A.E.C. report C/TN7.

TABLE 1

SPECIMEN COMPOSITIONS AND MEAN IRRADIATION TEMPERATURES

Sample No.	Basic Atom Ratio			Accelerated Atom Ratio			Composition Wt %			Volume % $(U,Th)Be_{13}$	$(U,Th)Be_{13}$ Particle Size (microns)	Mean Irradiation Temperature °C
	U	Th	Be	U	Th	Be	U	Th	Be			
1	1	30	4000	12	19	4000	6.5	10.2	83.3	11	100 – 150	520
2	,,	,,	,,	,,	,,	,,	,,	,,	,,	,,	,,	465
5	1	30	3000	12	19	3000	8.2	12.9	78.9	16	,,	490
6	,,	,,	,,	,,	,,	,,	,,	,,	,,	,,	,,	495
7	,,	,,	,,	,,	,,	,,	,,	,,	,,	,,	,,	435
8	,,	,,	,,	,,	,,	,,	,,	,,	,,	,,	,,	445
9	,,	,,	,,	,,	,,	,,	,,	,,	,,	,,	,,	505
10	,,	,,	,,	,,	,,	,,	,,	,,	,,	,,	,,	515
17	,,	,,	,,	14	17	3000	9.6	11.5	78.9	,,	2 – 50	435
18	,,	,,	,,	,,	,,	,,	,,	,,	,,	,,	,,	450
21	1	30	2000	12	19	2000	11.2	17.4	71.4	24	100 – 150	465
22	,,	,,	,,	,,	,,	,,	,,	,,	,,	,,	,,	505
25	1	30	1000	12	19	1000	17.4	27.1	55.5	46	,,	520
26	,,	,,	,,	,,	,,	,,	,,	,,	,,	,,	,,	530
29	1	30	3000	24	7	3000	16.45	4.7	78.8	16	,,	510
30	,,	,,	,,	,,	,,	,,	,,	,,	,,	,,	,,	500

TABLE 2

IMPURITY CONTENTS OF MATERIALS USED IN SPECIMEN PREPARATION

Material	Impurity Content, p.p.m.				
	Al	Si	Fe	H	Halogens
Beryllium	1060	90	740	N.D.	300
Uranium	N.D.	N.D.	N.D.	150	N.D.
Thorium	790	370	120	N.D.	N.D.

N.D. = Not Determined.

TABLE 3

OPTICAL MEASUREMENTS OF INTERMETALLIC COMPOUND PARTICLES

Nominal Particle Size Range	Length (μ)			Breadth (μ)			No. of Particles Examined
	Max	Min	Mean	Max	Min	Mean	
100 – 150 μ (–100, +150 mesh)	480	120	244	200	60	149	65
10 micron	60	3	14	42	1 – 2	9	40

TABLE 4

COMPOSITIONS OF INTERMETALLIC COMPOUNDS AS DETERMINED BY CHEMICAL ANALYSIS

Material	Nominal Atom Ratio	Composition from Chemical Analysis wt. %				Atom Ratio Calculated from Analytical Results	Stoichiometry
	U : Th : Be	%U	%Th	%Be	%O	U : Th : Be	
Composition A	12 : 19 : 403	26.2	37.9	31.8	0.4	13 : 19 : 410	$M Be_{12.8}$
Composition B	14 : 17 : 403	28.7	32.9	31.8	0.3	15 : 17 : 430	$M Be_{12.45}$
Composition C	24 : 7 : 403	50.6	16.3	32.1	0.4	21.5 : 7 : 355	$M Be_{12.45}$

TABLE 5

BURN–UPS IN IRRADIATED SPECIMENS

Specimen No.	From Low Power Flux Data		From Co Monitors		From Cs–137 Analysis		From Isotope Dilution Analysis	
	% Burn–up of U	Equivalent Burn–up	% Burn–up of U	Equivalent Burn–up	% Burn–up of U	Equivalent Burn–up	% Burn–up of U	Equivalent Burn–up
1	9.2	110	8.5	101				
2			8.5	101				
5	9.6	111	8.7	103				
6			8.3	99				
7	10.1	117	10.4	124	13.6	160	16.8	195
8			8.7	103				
9	10.6	123	5.5	65.5				
10			7.9	94				
17	10.6	123	6.9	96				
18			5.5	76.5				
21	10.0	117	–	–				
22			8.25	98				
25	8.4	97.5	7.1	84.5				
26			7.1	84.5				
29	8.4	195	8.7	207				
30			8.7	207	13.5	325	9.3	233

TABLE 6

FISSION PRODUCT GAS RELEASE

Specimen No.	Volume in ($cm^3 \times 10^{-5}$)								% Release								
	Kr				Xe				Kr				Xe				Mean
	83	84	85	86	131	132	134	136	82	84	85	86	131	132	134	136	
1	4	7	2	20	25	36	59	78	0.65	0.7	0.55	0.65	0.6	0.6	0.55	0.85	0.64
2	nil result																
5	nil result																
6	3	6	1	9	15	20	35	50	0.35	0.45	0.2	0.2	0.25	0.22	0.22	0.4	0.29
7	4	6	1	10	17	22	39	56	0.45	0.4	0.2	0.2	0.25	0.25	0.25	0.4	0.30
8	9	13	3	20	56	66	86	122	1.0	0.9	0.55	0.45	0.9	0.7	0.5	0.9	0.74
9	9	16	3	27	56	75	105	147	1.0	1.1	0.55	0.6	0.9	0.8	0.65	1.05	0.84
10	10	20	5	30	60	90	124	172	1.1	1.4	0.9	0.7	1.1	1.0	0.75	1.2	1.02
17	nil result																
18	nil result																
21	nil result																
22	17	27	7	45	85	118	180	220	1.4	1.4	0.45	0.7	1.0	0.9	0.8	1.2	0.98
25	nil result																
26	44	81	21	150	210	310	590	730	2.2	2.5	1.7	1.5	1.5	1.5	1.6	2.3	1.85
29	22	37	9	61	131	175	242	334	1.6	1.6	1.0	0.85	1.3	1.2	0.9	1.5	1.24
30	nil result																

TABLE 7

DENSITY AND DIMENSION CHANGES IN IRRADIATED SPECIMENS

Sample No.	Diameter (mean)			Height (mean)			Density Change from Metrology %	Displacement Density		
	Before cm	After cm	% Change	Before cm	After cm	% Change		Before g cm^{-3}	After g cm^{-3}	% Change
1	0.900	0.905	+ 0.55	1.806	1.813	+ 0.4	− 1.5	2.140	2.129	− 0.5
2	0.901	0.903	+ 0.2	1.806	1.813	+ 0.4	− 0.8	2.141	2.139	− 0.1
5	0.902	0.904	+ 0.2	1.804	1.814	+ 0.5	− 0.9	2.260	2.248	− 0.5
6	0.900	0.903	+ 0.3	1.806	1.811	+ 0.3	− 0.9	2.261	2.245	− 0.7
7	0.910	0.913	+ 0.4	1.807	1.820	+ 0.7	− 1.5	2.244	2.231	− 0.6
8	0.897	0.912	+ 0.3	1.807	1.809	+ 0.1	− 0.7	2.251	2.237	− 0.6
9	0.899	0.904	+ 0.4	1.802	1.810	+ 0.4	− 1.2	2.267	2.249	− 0.8
10	0.910	0.911	+ 0.1	1.806	1.810	+ 0.2	− 0.4	2.236	2.209	− 1.2
17	0.914	0.919	+ 0.6	1.806	1.818	+ 0.6	− 1.8	2.256	2.188	− 3.1
18	0.909	0.912	+ 0.3	1.807	1.810	+ 0.2	− 0.8	2.266	2.209	− 2.5
21	0.926	0.933	+ 0.8	1.804	1.822	+ 1.0	− 2.6	2.408	2.325	− 3.4
22	0.899	0.902	+ 0.3	1.807	1.812	+ 0.3	− 0.9	2.450	2.421	− 1.1
25	0.928	0.940	+ 1.35	1.807	1.830	+ 1.3	− 3.9	2.927	2.777	− 5.1
26	0.922	0.937	+ 1.8	1.807	1.831	+ 1.3	− 4.9	2.925	2.789	− 4.6
29	0.911	0.916	+ 0.6	1.806	1.818	+ 0.6	− 1.8	2.235	2.130	− 4.7
30	0.914	0.921	+ 0.8	1.806	1.819	+ 0.7	− 2.5	2.215	2.188	− 1.2

TABLE 8

DIMENSION AND DENSITY CHANGES IN UNIRRADIATED HEAT-TREATED CONTROL SPECIMENS

Specimen No.	Corresponding Irradiated Specimen	Diameter (mean)			Height (mean)			Density Change from Metrology %	Density (displacement)		
		Before cm	After cm	% Change	Before cm	After cm	% Change		Before $g\ cm^{-3}$	After $g\ cm^{-3}$	% Change
3	1	0.8992	0.9007	+ 0.17	1.7998	1.8059	+ 0.34	− 0.7	2.146	2.144	− 0.09
11	5	0.9004	0.9002	− 0.02	1.8050	1.8085	+ 0.19	− 0.15	2.243	2.243	0
12	5	−	0.8997	−	−	1.8062	−	−	2.252	2.242	− 0.44
13	5	−	0.9012	−	−	1.8110	−	−	2.261	2.259	− 0.09
19	17	0.9101	0.9106	+ 0.054	1.8057	1.8090	+ 0.182	− 0.3	2.226	2.217	− 0.40
23	23	0.9096	0.9103	+ 0.081	1.8021	1.8077	+ 0.31	− 0.5	2.427	2.410	− 0.70
27	25	0.9215	0.9228	+ 0.14	1.8070	1.8143	+ 0.4	− 0.7	2.852	2.853	+ 0.03
31	29	0.9103	0.9096	− 0.08	1.7993	1.8072	+ 0.44	− 0.3	2.245	2.236	− 0.4

TABLE 9

TOTAL FISSION GAS RELEASE, FISSION CONCENTRATION AND PER CENT. DENSITY CHANGE

Specimen No.	Total Gas Released ($cm^3 \times 10^{-5}$)	Irradiation Temperature °C	Volume Per Cent. of Fuel Phase	Fission Concentration Fission/cm^3	Density As-Fabricated g. cm^{-3}	Density After Irradiation g. cm^{-3}	Displacement Density Change %
				$\times 10^{-19}$			
26	2000	530	46	11.4	2.925	2.780	- 4.6
29	1010	510	16	8.4	2.235	2.130	- 4.7
22	700	505	24	7.45	2.450	2.421	- 1.1
10	510	515	16	5.25	2.356	2.209	- 1.2
9	438	505	16	5.25	2.267	2.249	- 0.8
8	375	445	16	5.05	2.251	2.237	- 0.6
1	231	520	11	3.72	2.140	2.129	- 0.5
7	155	435	16	5.05	2.244	2.231	- 0.6
6	140	445	16	4.83	2.261	2.245	-0.7

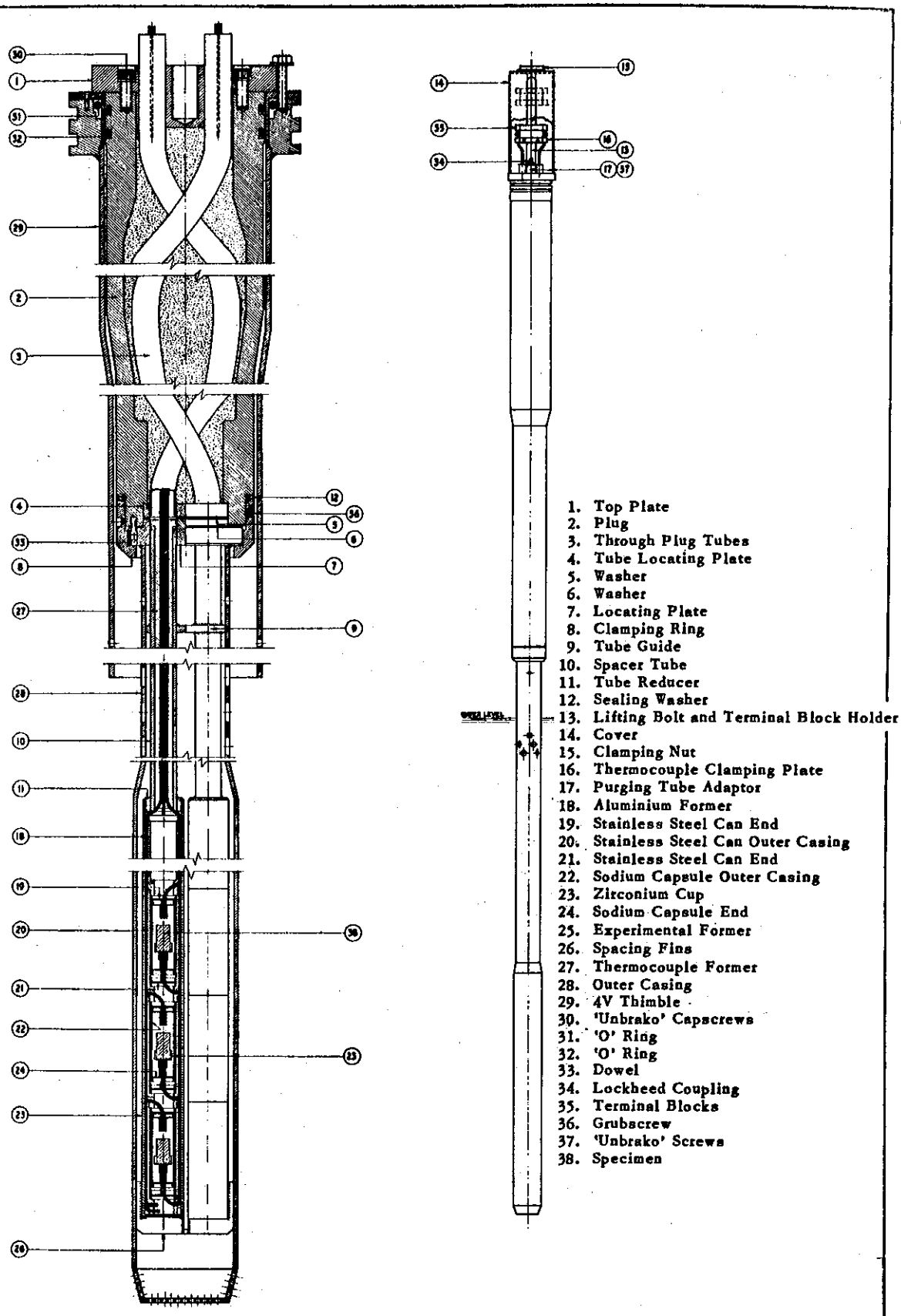

1. Top Plate
2. Plug
3. Through Plug Tubes
4. Tube Locating Plate
5. Washer
6. Washer
7. Locating Plate
8. Clamping Ring
9. Tube Guide
10. Spacer Tube
11. Tube Reducer
12. Sealing Washer
13. Lifting Bolt and Terminal Block Holder
14. Cover
15. Clamping Nut
16. Thermocouple Clamping Plate
17. Purging Tube Adaptor
18. Aluminium Former
19. Stainless Steel Can End
20. Stainless Steel Can Outer Casing
21. Stainless Steel Can End
22. Sodium Capsule Outer Casing
23. Zirconium Cup
24. Sodium Capsule End
25. Experimental Former
26. Spacing Fins
27. Thermocouple Former
28. Outer Casing
29. 4V Thimble
30. 'Unbrako' Capscrews
31. 'O' Ring
32. 'O' Ring
33. Dowel
34. Lockheed Coupling
35. Terminal Blocks
36. Grubscrew
37. 'Unbrako' Screws
38. Specimen

FIGURE 1 GENERAL ARRANGEMENT OF IRRADIATION RIG

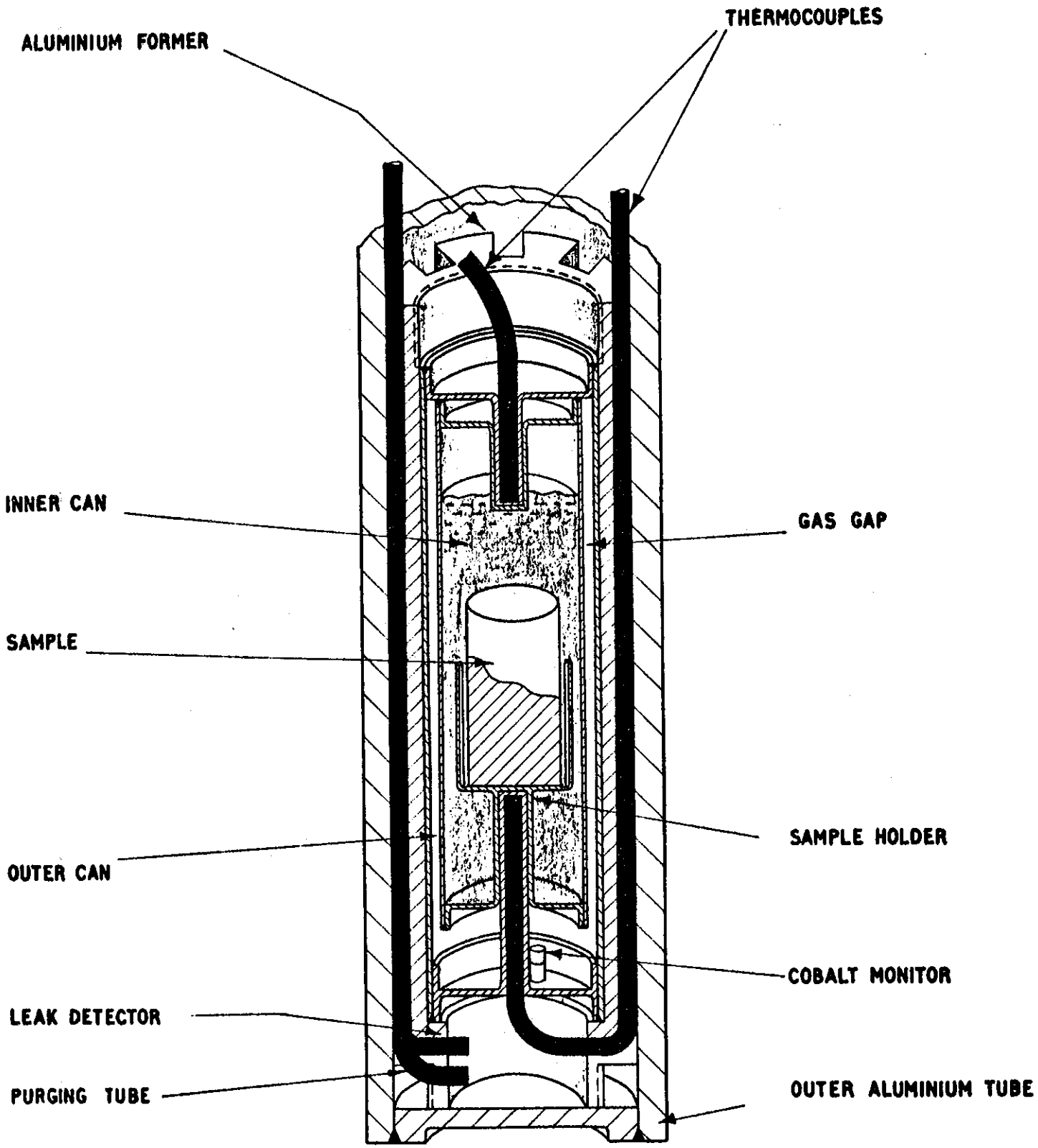

FIGURE 2 SCHEMATIC SECTION OF IRRADIATION CAN

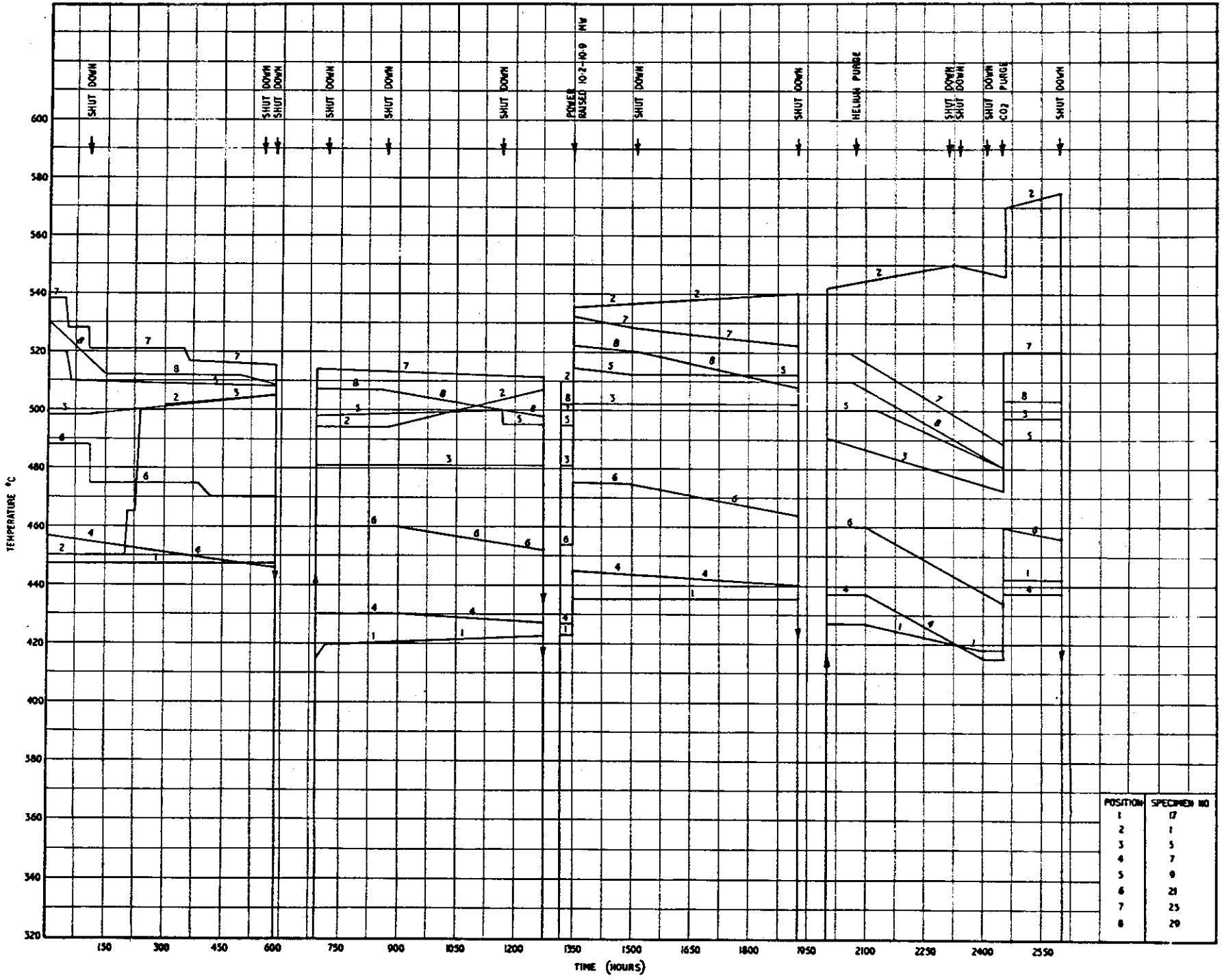

FIGURE 3a X-11 TEMPERATURE CHART – STRINGER A

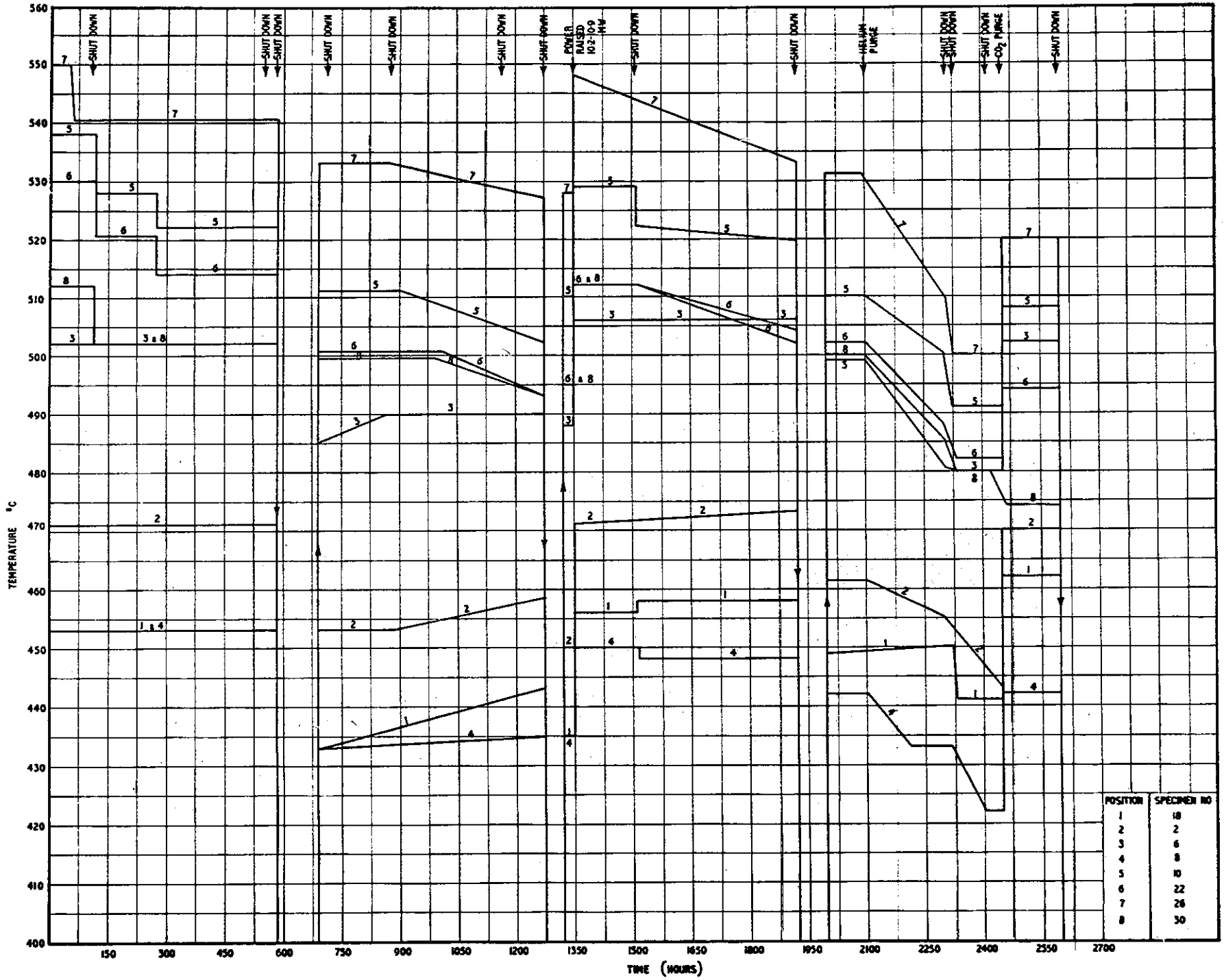

FIGURE 9b X-11 TEMPERATURE CHART-STRINGER B

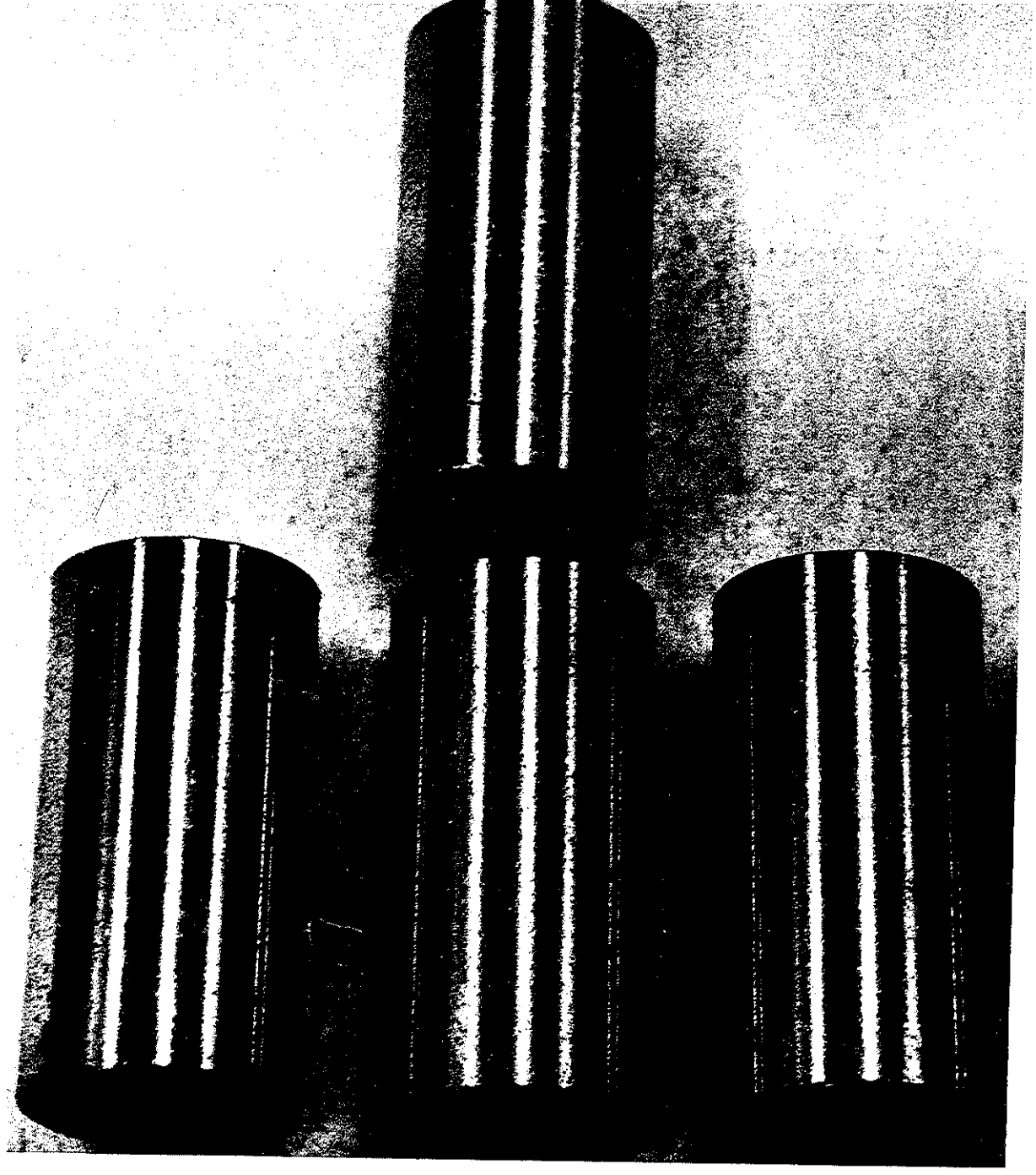

X 4 approx.

FIGURE 4 PHOTOGRAPH OF TYPICAL SPECIMENS BEFORE IRRADIATION

X 12

FIGURE 5a PHOTOGRAPH OF SURFACE OF IRRADIATED SPECIMEN 26 SHOWING SURFACE ROUGHENING DUE TO SODIUM ATTACK

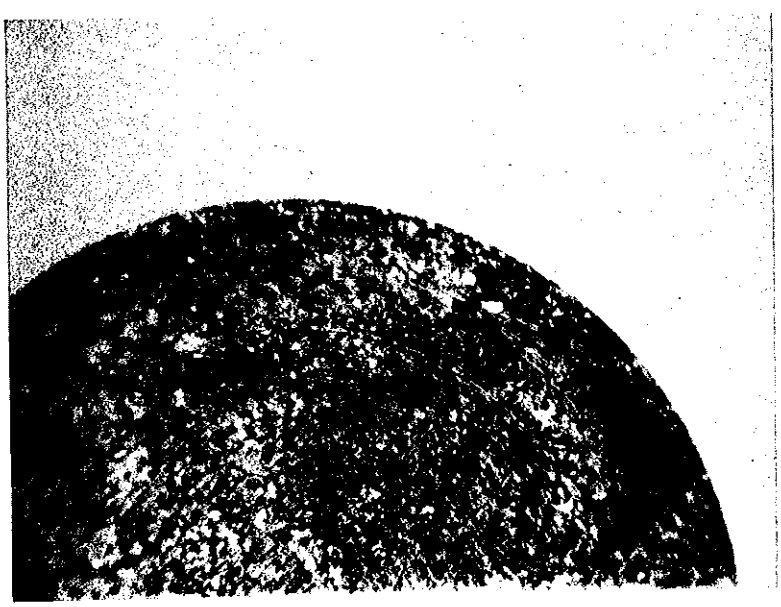

X 12

FIGURE 5b PHOTOGRAPH OF THE SURFACE OF SPECIMEN 27

(Thermal History and Exposure to Sodium as for Specimen 26 but no Irradiation)

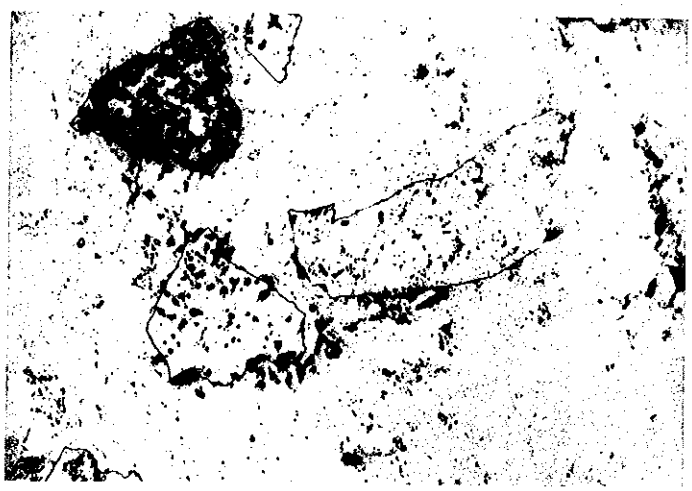

X 160

FIGURE 6 SPECIMENS 1 – 4

X 160

FIGURE 7 SPECIMENS 5 – 16

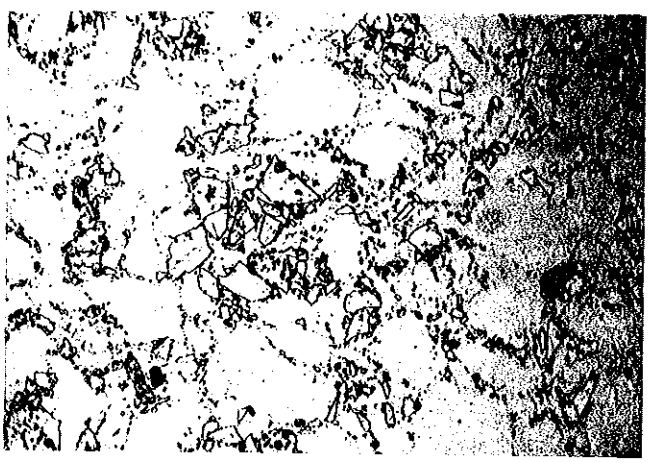

X 160

FIGURE 8 SPECIMENS 17–20

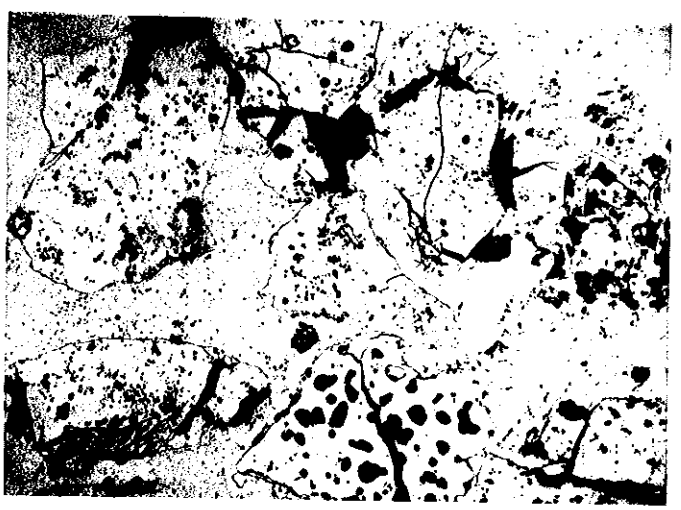

X 160

FIGURE 9 SPECIMENS 21 – 24

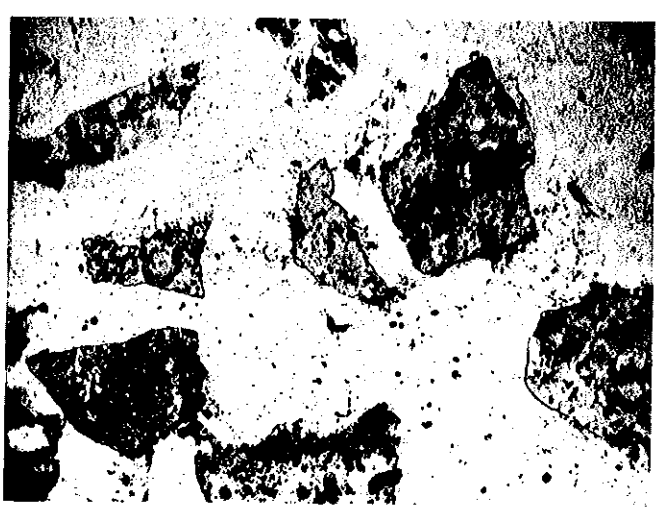

X 160

FIGURE 10 SPECIMENS 25 – 28

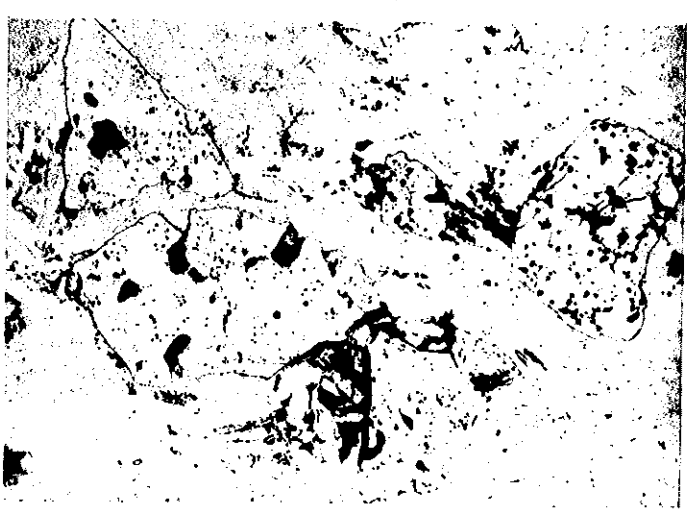

X 160

FIGURE 11 SPECIMENS 29 – 32

FIGURES 6 – 11 MICROSTRUCTURE OF AS–FABRICATED SPECIMENS 1 – 32

X 160

(a) Transverse

X 160

(b) Longitudinal

FIGURE 12 MICROSTRUCTURE OF IRRADIATED SPECIMEN 2

X 160

(a) Transverse

X 160

(b) Longitudinal

FIGURE 13 MICROSTRUCTURE OF IRRADIATED SPECIMEN 6

X 160

(a) Transverse

X 160

(b) Longitudinal

FIGURE 14 MICROSTRUCTURE OF IRRADIATED SPECIMEN 17

X 160

(a) Transverse

X 160

(b) Longitudinal

FIGURE 15 MICROSTRUCTURE OF IRRADIATED SPECIMEN 21

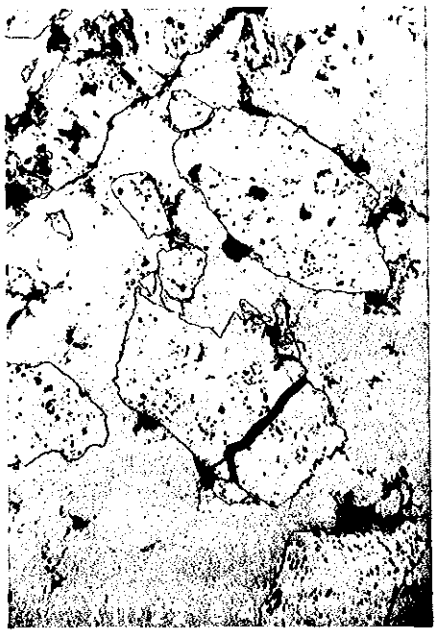

X 160

(a) Transverse

X 160

(b) Longitudinal

FIGURE 16 MICROSTRUCTURE OF IRRADIATED SPECIMEN 22

X 160

(a) Transverse

X 160

(b) Longitudinal

FIGURE 17 MICROSTRUCTURE OF IRRADIATED SPECIMEN 25

X 160

(a) Transverse

X 160

(b) Longitudinal

FIGURE 18 MICROSTRUCTURE OF IRRADIATED SPECIMEN 29

X 160

(a) Transverse

X 160

(b) Longitudinal

FIGURE 19 MICROSTRUCTURE OF IRRADIATED SPECIMEN 30